Drosophila Calmodulin Mutants With Specific Defects in the Musculature or in the Nervous System

Bo Wang,*,[1] Kathleen M. C. Sullivan† and Kathy Beckingham*,[2]

**Department of Biochemistry and Cell Biology, Rice University, Houston, Texas 77005 and †Howard Hughes Medical Institute and Department of Molecular and Cell Biology, University of California, Berkeley, California 94702*

Manuscript received March 21, 2003
Accepted for publication July 22, 2003

ABSTRACT

We have studied lethal mutations in the single calmodulin gene (*Cam*) of Drosophila to gain insight into the *in vivo* functions of this important calcium sensor. As a result of maternal calmodulin (CaM) in the mature egg, lethality is delayed until the postembryonic stages. Prior to death in the first larval instar, *Cam* nulls show a striking behavioral abnormality (spontaneous backward movement) whereas a mutation, Cam^{7}, that results in a single amino acid change (V91G) produces a very different phenotype: short indented pupal cases and pupal death with head eversion defects. We show here that the null behavioral phenotype originates in the nervous system and involves a CaM function that requires calcium binding to all four sites of the protein. Further, backward movement can be induced in hypomorphic mutants by exposure to high light levels. In contrast, the V91G mutation specifically affects the musculature and causes abnormal calcium release in response to depolarization of the muscles. Genetic interaction studies suggest that failed regulation of the muscle calcium release channel, the ryanodine receptor, is the major defect underlying the Cam^{7} phenotype.

THE small calcium sensor protein calmodulin (CaM) is one of the major mediators of the complex interactions that underlie calcium regulation (see Van Eldik and Watterson 1998 for review). CaM is present in all eukaryotic cells and is highly conserved across evolutionary orders. Two pairs of EF-hand-type calcium-binding sites are present in each of its two globular domains and conformational changes produced by calcium binding dramatically alter the target interaction properties of the protein. CaM thus converts changes in calcium levels into changes in target activity.

The large array of CaM targets identified to date includes protein kinases, the ubiquitous protein phosphatase calcineurin, adenyl cyclase, cyclic nucleotide phosphodiesterase, and cytoskeletal proteins such as spectrin and adducin. More recently, calcium channels and calcium-regulated channels have proved to be CaM targets (reviewed in Saimi and Kung 2002). These include ryanodine receptor (RyR) channels and L-type voltage-gated dihydropyridine receptor (DHPR) channels of muscle tissues.

In vitro experimentation is elucidating the molecular detail of CaM interactions with individual targets. However, given that CaM plays a central role in coordinating calcium responses, there are aspects of function that can be revealed only by *in vivo* genetic studies. Genetic studies to date in unicellular eukaryotes demonstrate this point. In Paramecium, for example, Kung and coworkers uncovered striking effects of CaM mutations on avoidance responses, which entail plasma membrane depolarization and a bout of backward swimming (Saimi and Kung 1987). Surprisingly, mutations in the N- or C-terminal globular domains of CaM produce opposing effects. Mutations in the C-terminal domain show spontaneous or exaggerated backward swimming due to loss of a restorative, repolarizing, Ca^{2+}-dependent K^{+} current. In contrast, mutations in the N-terminal domain give curtailed avoidance responses due to loss of a depolarizing Ca^{2+}-dependent Na^{+} current (Kink *et al.* 1990). These studies first demonstrated a functional partitioning inherent in the domain structure of CaM (Van Houten *et al.* 1977; Ling *et al.* 1994).

More recent work with *Saccharomyces cerevisiae* has also provided insights that could come only from *in vivo* studies. Thus, genetic rescue experiments with versions of CaM defective in calcium binding (Geiser *et al.* 1991) provided the first evidence that Ca^{2+}-free CaM (apoCaM) performs important functions in the cell. Further, systematic mutation of the individual phenylalanines of *S. cerevisiae* CaM (Ohya and Botstein 1994) led to identification of four intragenic complementation groups and the realization that different regions of CaM are critical for different targets and different intracellular processes (reviewed in Cyert 2001).

We have used a genetic approach to address CaM function in the complex multicellular organism, *Drosophila melanogaster*. In contrast to other genetically tractable animals and plants, Drosophila contains only one

[1]*Present address:* Union Biometrica, Somerville, MA 02143.

[2]*Corresponding author:* Department of Biochemistry and Cell Biology, MS-140 Rice University, P.O. Box 1892, Houston, TX 77251. E-mail: kate@bioc.rice.edu

gene (*Cam*) encoding CaM (Doyle *et al.* 1990), thus eliminating potential problems with functional substitution. We have generated the following classes of Drosophila *Cam* mutations: (i) RNA nulls that produce no zygotic CaM protein (Heiman *et al.* 1996), (ii) hypomorphs that produce decreased levels of CaM (Scott *et al.* 1997), and (iii) point mutations that alter individual amino acids within the protein (Nelson *et al.* 1997).

None of these *Cam* mutations affect embryonic development, reflecting our discovery that maternal CaM persists until immediately before hatching (Heiman *et al.* 1996; B. F. Andruss and K. Beckingham, unpublished results). No zygotic protein is produced until late in embryogenesis despite early zygotic transcription of *Cam* in neural lineages (Kovalick and Beckingham 1992). As a consequence, even RNA nulls hatch as morphologically normal first instar larvae (Heiman *et al.* 1996). Distinct phenotypes are detected among the *Cam* mutants, however. Although *Cam* nulls die in first instar, they show striking behavioral abnormalities. These include spontaneous backward movement, reminiscent of Paramecium CaM mutants, and increased head swinging (Heiman *et al.* 1996). None of five point mutations affecting the CaM protein coding sequence (Nelson *et al.* 1997) show these defects, but several show distinctive alternative phenotypes. For example, Cam^{3c1}, which encodes a CaM altered in calcium-binding site 1, permits survival of some morphologically normal adults but, uniquely, produces enhanced excitability of the larval neuromuscular junction (Arredondo *et al.* 1998).

Only one of the point mutations isolated, Cam^{7}, which encodes the mutant CaM V91G, produces a morphological phenotype. Cam^{7} animals form aberrant pupal cases with indentations at the larval segment boundaries, giving them a "Michelin man" appearance. The mutants all die as pupae, sometimes with "inside-out" heads buried in the thorax (Nelson *et al.* 1997). We have investigated the underlying defects in both *Cam* null and Cam^{7} animals. We have demonstrated the neural origin of the backward movement of the null and the influence of light on this phenotype. In contrast, most of the Cam^{7} phenotype is muscle specific and associated with altered-muscle calcium fluxes. Genetic interaction experiments suggest that the ryanodine receptor is one of the major muscle targets affected by this mutation.

MATERIALS AND METHODS

Mutations: The following mutations were used: Cam^{n339}, recessive RNA null mutation (Heiman *et al.* 1996); Cam^{7}, recessive ethyl methanesulfonate mutation (Nelson *et al.* 1997); Cam^{352}, recessive hypomorph, generated by excision of a *P* element in 5′ flanking DNA (Scott *et al.* 1997); Cam^{3909}, recessive hypomorph generated by a P insertion 60 bp 5′ of the transcription start site (Harvie *et al.* 1998); Ryr^{16}, recessive mutation of the ryanodine receptor gene (*Ryr*; Sullivan *et al.* 2000); *Df(2R)H3E1*, deficiency with breakpoints at 44D1–4 and 44F12 (Bloomington Stock Center); $Ca\text{-}\alpha 1D^{X7}$, embryonic lethal *Ca-α1D* mutation (Eberl *et al.* 1998); $Ca\text{-}\alpha 1D^{AR66}$, hypomorphic *Ca-α1D* mutation (Eberl *et al.* 1998; Ren *et al.* 1998); and cn^{1}, *cinnabar* (Bloomington Stock Center).

Gal4 lines: We used the following Gal4 lines: *24B-Gal4*, P{GawB}how^{24B}, an insertion into *held out wings* that expresses Gal4 in muscle (Brand and Perrimon 1993); *elav-Gal4*, Gal4 expressed under the *elav* promoter in neurons at all developmental stages (Yao and White 1994); and *sca-Gal4*, Gal4 expressed under the control of the *scabrous* promoter in the central nervous system and the peripheral nervous system before embryonic stage 14 (Mlodzik *et al.* 1990).

UAS and other lines: *UAS-CaM, UAS-B12Q, UAS-B34Q, UAS-B1234Q,* and *UAS-V91G* constructs were generated in the UAS vector of Brand and Perrimon (1993) and expressed the following CaMs, respectively: wild-type CaM, CaM with Ca^{2+}-binding sites 1 and 2 disabled, CaM with binding sites 3 and 4 disabled, CaM with all four binding sites disabled, and finally, V91G mutant CaM (Wang *et al.* 2002). Stocks carrying UAS-aequorin, UAS-lacZ, and UAS-green fluorescent protein (GFP) are described in Rosay *et al.* (1997), Brand and Perrimon (1993), and Brand (1995), respectively. A stock carrying lacZ under the control of the myosin heavy chain promoter (MHC-lacZ) was obtained from Sanford Bernstein (Hess *et al.* 1989).

Stocks and crosses: All *Cam* mutations were kept in *y w; Cam/ CyO*(y^{+}) stocks so that *Cam* mutant combinations could be selected from crosses of such stocks. The required larvae were identified by y^{-} mouth hooks. To examine the Cam^{7} hemizygous phenotype, the following cross was used: *y w;* Cam^{7}*/CyO*(y^{+}) × *y w;* Cam^{n339}*/CyO*(y^{+}). For the *Cam* null phenotype, homozygous Cam^{n339} larvae were examined.

To express UAS constructs with a chromosome 3 Gal4 driver in the Cam^{7} or Cam^{n339} backgrounds, stocks for the following cross were generated: *y w;* $Cam^{7/n339}$*/CyO*(y^{+})*; UAS-test* × *y w;* Cam^{n339}*/CyO*(y^{+})*; Gal4driver*. For chromosome 2 Gal4 drivers, the Gal4 insertion was introduced onto the Cam^{n339} chromosome by recombination and stocks were prepared for the following cross: *y w;* $Cam^{7/n339}$*/CyO*(y^{+})*; UAS-Cam* × *y w;* Cam^{n339}*, Gal4driver / CyO*(y^{+}).

Ryr, Ca-α1D, and *cinnabar* (*cn*) mutations were recombined onto the Cam^{7} chromosome. Putative recombinant chromosomes were tested by backcrossing to confirm the presence of both mutations. For Ryr^{16}, which gave an unexpected phenotype (see RESULTS), the Cam^{7} mutation was reisolated from one recombinant chromosome to confirm its presence on the double-mutant chromosomes.

Larval/pupal studies: First instar larvae were collected, sorted by mouth hook color, and transferred to food vials (30 per vial). Larvae were kept at 25° in a 12-/12-hr light-dark cycle. Pupal lengths and widths were measured under a dissecting microscope. Statistical analyses were performed using Statview software (Abacus Concepts, Berkeley, CA).

Behavioral studies: *Larval locomotion assay:* Larvae were placed on moist 1% agarose plates and left for a 1-min adjustment period. The number of body-wall contractions (BWC) in a 1-min interval was recorded for each animal. A total of 8000–10,000 lx was used for strong light, and 400–500 lx was used for low light.

Adult behavioral tests: Flies used for behavioral tests were collected immediately after eclosion and aged individually in vials for 3 days before testing. Climb, flight, and vortexing tests described previously (Nelson *et al.* 1997) were used with little modification.

For mating assays, male flies were placed individually in vials with two virgin Oregon-R females and observed for 1 hr. Time spent performing various elements of the mating ritual was recorded.

Larval body-wall muscle staining: Third instar larvae were im-

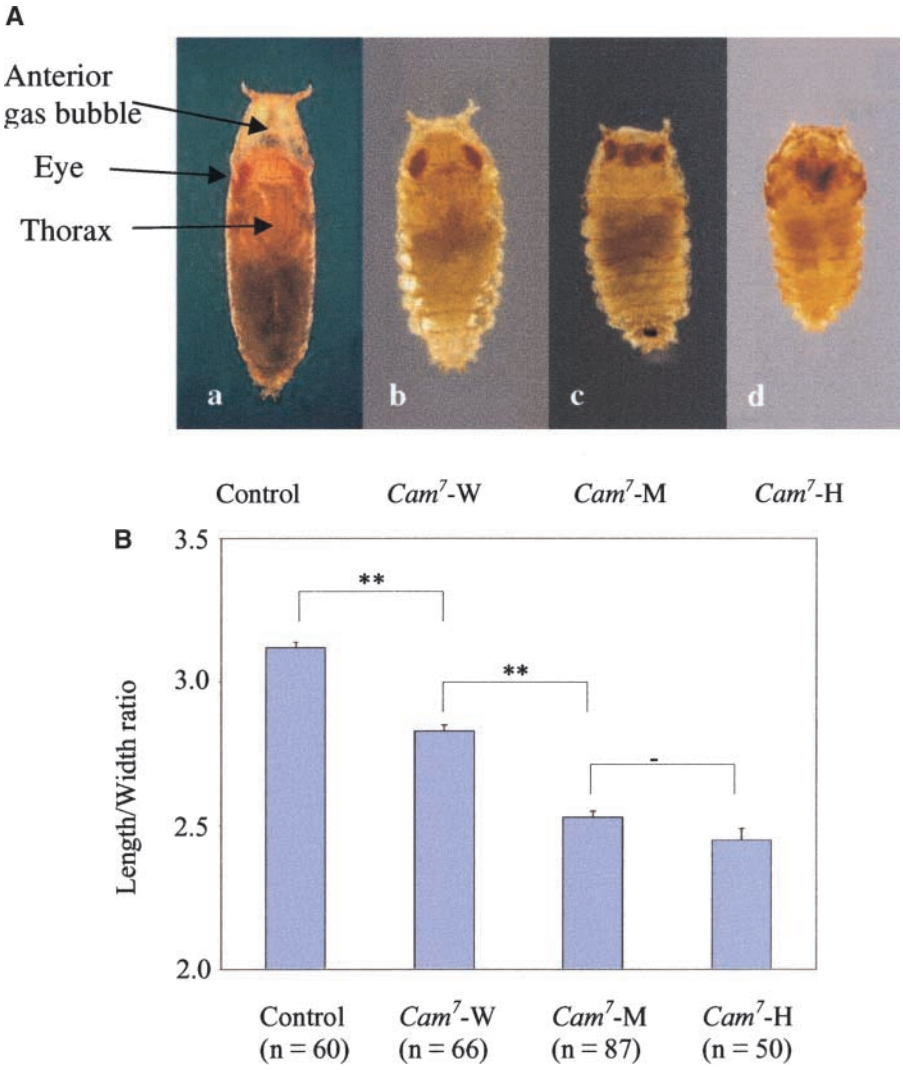

FIGURE 1.—Aberrant pupal cases and pharate adult head structures in *Cam*^{7} mutants. (A) The *Cam*^{7} mutation leads to the formation of "Michelin man" pupal cases (b–d), which are shorter than wild type (a) and have highly indented rings around the body. *Cam*^{7} pharate adults display three types of head structures: well-formed (*Cam*^{7}-W, b); malformed (*Cam*^{7}-M, c), and "inside-out" within the thorax as a result of failed head eversion (*Cam*^{7}-H, d). The adult head is formed by eversion of the head sac into an anterior gas bubble (a). The presence of a gas bubble is variable in *Cam*^{7} and does not correlate with the degree of failure of head eversion. (B) Correlation of pupal length:width ratio with the degree of head abnormality in *Cam*^{7} pharate adults. The more severe head defects in *Cam*^{7} animals are associated with shorter pupal cases. *Cam*^{7}-W, *Cam*^{7}-M, and *Cam*^{7}-H as in A. *n*, number of animals measured. *P* values for the length:width ratios: between control and *Cam*^{7}-W, $P < 0.0001$ (**); between *Cam*^{7}-W and *Cam*^{7}-M or *Cam*^{7}-H, $P < 0.0001$ (**); between *Cam*^{7}-M and *Cam*^{7}-H, $P = 0.07$ (–). Genotypes: control, *y w; Cam*^{n339}/+. *Cam*^{7}, *y w; Cam*^{n339}/*Cam*^{7}.

mobilized and their muscles relaxed with ether vapor. Pinned larvae were dissected in Ca^{2+}-free saline (130 mM NaCl, 5 mM KCl, 36 mM sucrose, 4 mM $MgCl_2$, 0.5 mM EGTA, 5 mM HEPES, pH 7.3) to minimize contraction. Larvae were cut along the dorsal midline and internal organs were removed. The cleaned body walls were fixed in PBS (137 mM NaCl, 2.68 mM KCl, 10.14 mM Na_2HPO_4, 1.76 mM KH_2PO_4, pH 7.5) containing 4% paraformaldehyde for 30 min and the muscles were stained with rhodamine-phalloidin (10 units/ml; Molecular Probes, Eugene, OR) for 1 hr in PBX (PBS + 0.15% Triton X-100) with gentle rotation. After several rinses in PBX, the muscles were inspected by fluorescence microscopy.

K-contracture and aequorin luminescence recording: Third instar larvae were relaxed on ice, pinned on glass plates using magnetic needles, and opened along the dorsal midline in bathing solution (140 mM NaCl, 2 mM KCl, 5 mM $CaCl_2$, 1 mM $MgCl_2$, 4 mM $NaHCO_3$, 5 mM trehalose, 100 mM sucrose, 5 mM HEPES, pH 7.0), modified from STEWART *et al.* (1994). After removal of internal organs, the body wall was incubated with coelenterazine (0.1 μg/μl; Molecular Probes) in bathing solution for 15 min in the dark with rotation. The body wall was then washed in bathing solution and transferred to the luminometer (Model TD-20e, Turner) chamber in a volume of 10 μl. K-contracture was induced by injection of 200 μl high-K solution (142 mM KCl, 5 mM $CaCl_2$, 1 mM $MgCl_2$, 4 mM $KHCO_3$, 5 mM trehalose, 100 mM sucrose, 5 mM HEPES, pH 7.0). Aequorin luminescence was collected using Black Night software and processed by Excel. To compensate for variation in expression of aequorin in individual larvae, a baseline was calculated for each animal by averaging the signal obtained during a 30-sec period before adding the high-K solution and was used to normalize the signal after depolarization.

RESULTS

Developmental and behavioral defects of the *Cam*^{7} mutant: The *Cam*^{7} phenotype was studied in the hemizygous condition. *Cam*^{7} larvae are morphologically normal and show normal forward locomotion with no spontaneous backward movement. But they are sluggish, with a BWC rate about one-third that of controls. The most striking problem occurs at pupariation when a severe morphological phenotype arises. As described previously (NELSON *et al.* 1997; WANG *et al.* 2002), pupal cases with deep indentations at the larval segment boundaries are produced (Figure 1A, b–d). Control larvae decrease their body length by one-third at pupariation, whereas we determined that, on average, *Cam*^{7} larvae decrease in

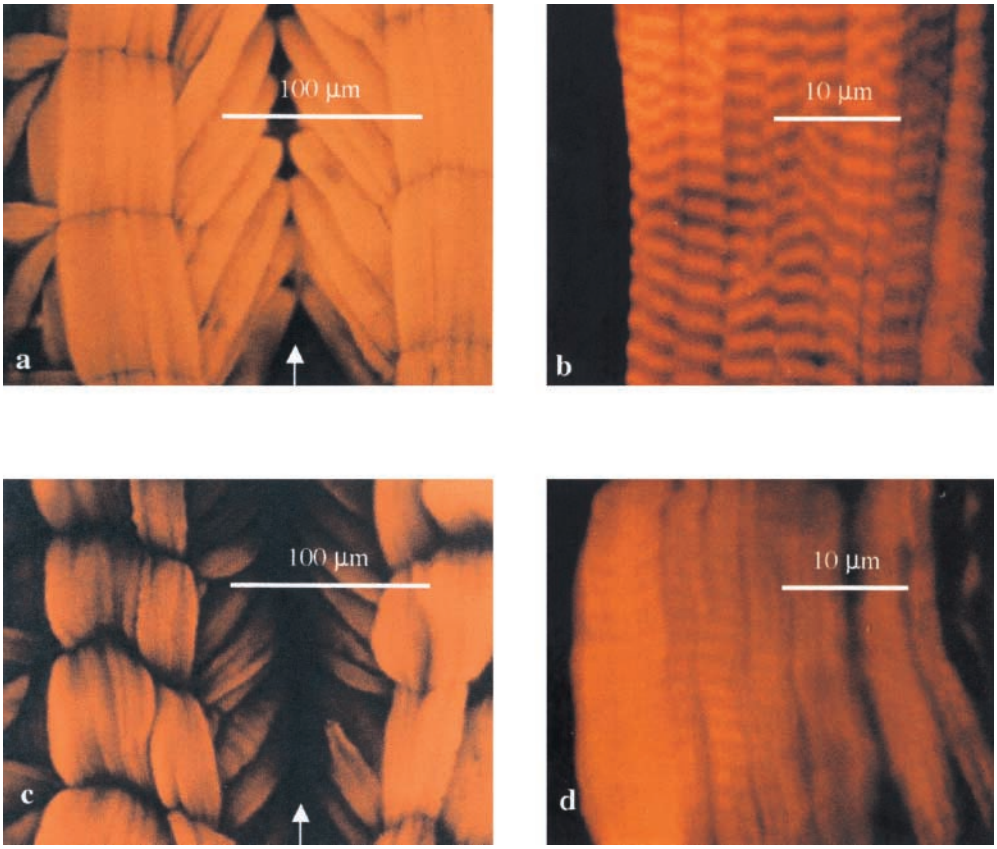

FIGURE 2.—Altered body-wall muscles in *Cam*^{7} mutant larvae. Rhodamine-phalloidin staining (see MATERIALS AND METHODS) of the larval body-wall muscles in wandering third instar larvae. Larvae were relaxed with ether prior to staining. Views of the internal ventral surface of the longitudinal muscles at ×10 (a and c) and ×63 (b and d) magnification. (a and b) Wild type. (c and d) *Cam*^{7}. The muscles of the *Cam*^{7} mutant appear "bunched" and the alignment of sarcomere repeats is lost in some muscles. Arrow indicates ventral midline.

length by 50%. Measurements of length:width ratios for control and *Cam*^{7} pupal cases (Figure 1B) confirmed that only the long axis of the body is abnormally compressed.

One possible explanation is that the longitudinal body-wall muscles of *Cam*^{7} animals are hypercontracted during pupariation. Consistent with this possibility, wandering third instar *Cam*^{7} larvae grow progressively incapable of relaxing at the end of each body-wall contraction and show increasing stiffness during locomotion. Examination of third instar body-wall muscles revealed that, despite artificial relaxation with ether, all mutant animals had groups of longitudinal muscles with a "bunched" appearance (Figure 2c) that showed structural disorganization and misaligned myofibrils (Figure 2d). These abnormalities suggest muscle degeneration, possibly as a result of hypercontraction.

Cam^{7} mutant pupae never eclose, but most develop into pharate adults with head defects. The adult head is formed from a head sac that is everted from the thorax into an anterior gas bubble ~10 hr after pupariation. Examination revealed three categories of heads among *Cam*^{7} pharate adults, each approximately equally represented (Table 2): (i) normal heads with no obvious defects (W class; Figure 1A, b), (ii) malformed heads (M class) that are partially everted (Figure 1A, c), and (iii) "inside-out" heads (H class; Figure 1A, d). Inside-out heads arise when head eversion fails completely and development proceeds in a noneverted head sac buried in the thorax.

Head eversion entails strong contractions by residual larval abdominal muscles. From videorecordings we determined that in all *Cam*^{7} mutant larvae, these contractions were weak and poorly synchronized or absent and often failed to give complete head eversion. Thus, failure of the residual larval muscles probably represents the major cause of the *Cam*^{7} head eversion defects. We found a correlation in the *Cam*^{7} pupae between length:width ratios and the three classes of pupal heads (Figure 1B). Thus, *Cam*^{7} pharate adults with normal heads have longer pupal cases than those with malformed or noneverted heads. This correlation suggests that both parameters reflect the degree of severity of the *Cam*^{7} defects.

It could be argued that the *Cam*^{7} mutant V91G CaM is less stable than wild-type CaM and that the phenotype simply reflects low levels of CaM. However, examination of the *Cam*^{352} mutant, which has severely decreased levels of CaM (SCOTT *et al.* 1997), discounted this possibility. Like *Cam*^{7}, *Cam*^{352} produces larval sluggishness and 100% pupal lethality. However, the *Cam*^{352} pupal cases are normal and the animals die as pharate adults with no head defects.

Rescue of the *Cam*^{7} lethality and pupariation defects by expression of exogenous wild-type CaM in the musculature: All aspects of the *Cam*^{7} phenotype suggest that muscle function, or neural control of muscle function,

TABLE 1

Rescue of *Cam^7* lethality by muscle-specific expression of wild-type CaM

Genotype	No. of first instar larvae collected	Larvae that puparite (%)	Larvae that eventually eclose as adults (%)
Cam$^+$	87	97.7	97.7
Cam^7	90	78.9	0
Cam^7 + muscle Cam$^+$	60	91.7	88.3
Cam^7 + neural(e) Cam$^+$	60	85.0	0
Cam^7 + neural(s) Cam$^+$	60	83.3	0

Cam$^+$, y w; Cam^7/+. Cam^7, y w; Cam^{n339}/Cam^7; 24B-Gal4/+. Cam^7 + muscle Cam$^+$, y w; Cam^{n339}/Cam^7; 24B-Gal4/UAS-CaM. Cam^7 + neural(e) Cam$^+$, y w; Cam^{n339} elav-Gal4/Cam^7; +/UAS-CaM. Cam^7 + neural(s) Cam$^+$, y w; Cam^{n339} sca-Gal4/Cam^7; +/UAS-CaM.

is specifically affected by the mutation. To address these possibilities, we expressed wild-type CaM in either the muscles or the nervous system using the Gal4-UAS system (Brand and Perrimon 1993). For muscle-specific expression we used the 24B-Gal4 driver (Brand and Perrimon 1993) and for neurons we expressed Gal4 under the control of promoters from (i) *elav* (*elav*-Gal4; Yao and White 1994) or (ii) *scabrous* (*sca*-Gal4; Mlodzik *et al.* 1990).

Expressing wild-type CaM with the 24B-Gal4 driver rescues the lethality and pupariation defects caused by the *Cam^7* mutation (Table 1; see also Wang *et al.* 2002). The rescued *Cam^7* larvae form pupal cases that are morphologically wild type and have more normal length:width ratios. Almost all of the rescued pupae eclose as adults and no aberrant pharate head structures are found. In contrast, expressing wild-type CaM specifically in the nervous system with either neural driver failed to rescue the lethality and the pupariation defects. Therefore, these aspects of the *Cam^7* phenotype specifically originate in the muscles, not in the nervous system (Table 1). However, the sluggish larval locomotion was incompletely rescued by either muscle or neural expression of CaM (Figure 3), suggesting a more generalized origin. Both *Cam* null and *Cam^{352}* mutant larvae also show larval sluggishness.

Interestingly, *Cam^7* mutant animals rescued to adulthood by expression of wild-type CaM in the muscles (rescued adults) were behaviorally abnormal. They failed to climb after being gently knocked to the bottom of a vial and showed poor flight and a reduced ability to right themselves after brief vortexing. In addition, rescued males, but not females, showed defective mating behavior. Initial stages of male courtship were normal, but, whereas wild-type males could penetrate females successfully after a few attempts, the rescued males could not achieve junction despite repeated mounting. For the Drosophila male to bring his genitalia into the correct position for intromission, he must bend his abdomen into a strongly curved position. The rescued males could not bend their abdomens sufficiently to achieve penetration.

The aberrant behaviors in rescued *Cam^7* adults could arise from two sources: (i) defects present in nonmuscle tissues in adults or, given that the adult expression pattern of 24B-Gal4 is uncharacterized, (ii) inadequate Gal4 expression from the 24B driver in adult muscles. This latter possibility seemed relevant to the male mating problem because the male-specific abdominal Muscles of Lawrence are required for abdominal bending during copulation. We compared the expression of the 24B-Gal4 line (using UAS-GFP and UAS-lacZ) to that of an MHC-lacZ construct in male abdominal muscles. MHC-lacZ gave strong expression in both the somatic and male-specific muscles. However, 24B-Gal4-induced expression was weak in the abdominal dorsal muscles and was not detectable in the Muscles of Lawrence. In contrast, 24B-Gal4 gave strong expression in adult leg muscles (data not shown). Therefore, the abnormal male mating behavior probably reflects inadequate expression in the required muscles.

Partial rescue of the *Cam^7* phenotype by a ryanodine receptor mutation: The aspects of the *Cam^7* phenotype that are unique to this *Cam* mutation arise specifically in the musculature and are (i) the permanent hypercontraction of the longitudinal body muscles at pupariation and (ii) the subsequent failure of the residual body-wall muscles during head eversion. This combination of defects is unprecedented in Drosophila. Failed head eversion due to abdominal muscle defects is also seen for mutations associated with the ecdysone pulses that orchestrate the puparial and pupal molts (Hadorn and Gloor 1943; Chadfield and Sparrow 1985; Fletcher *et al.* 1995; Hewes *et al.* 2000). In these mutants, muscle failure probably reflects premature death of the larval muscles (Fletcher *et al.* 1995; Hewes *et al.* 2000). However, none of these mutants show the hypercontraction at pupariation seen in *Cam^7* animals.

Although we could find no other Drosophila mutations producing hypercontraction at pupariation, we discovered a strikingly similar pharmacological "phenocopy" in the related Dipteran *Sarcophaga bullata.* Injection of ryanodine immediately prior to pupariation (Zdarek and Fraenkel 1972; Zdarek *et al.* 1979) pro-

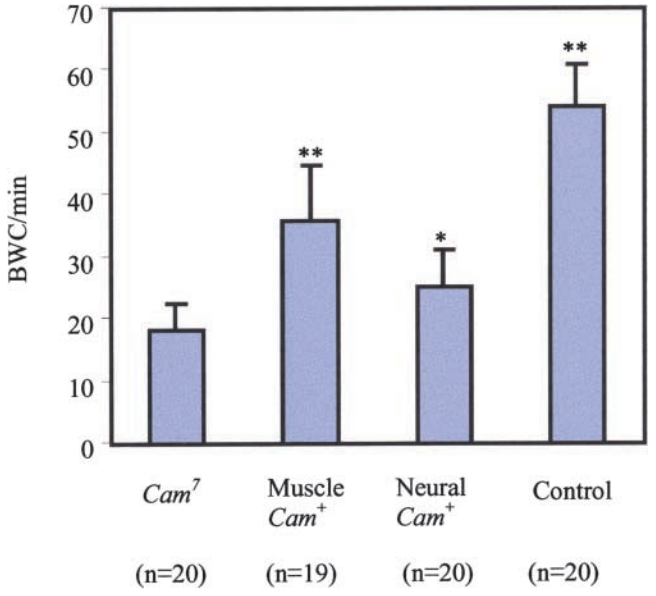

Figure 3.—Effects of expressing wild-type CaM in neural or muscle tissue upon the BWC rate of *Cam*^{7} larvae. Expression of wild-type CaM in the musculature of *Cam*^{7} mutants produces a partial, statistically significant rescue of locomotor activity; expression of CaM in the nervous system produces a smaller but still statistically significant enhancement of locomotion rate. *Cam*^{7}, *y w*; *Cam*^{7}/*Cam*^{n339}; muscle, *y w; Cam*^{7}/*Cam*^{n339}*; 24B-Gal4/UAS-CaM*; neural, *y w; Cam*^{7}/*Cam*^{n339} *elav-Gal4 ; +/UAS-CaM*; control, heterozygous siblings of the *Cam*^{7} mutant larvae for each cross whose second chromosome pair are *Cam*^{7}/+ or *Cam*^{n339}/+; *n*, number of larvae assayed. Error bar, standard deviation. *$P < 0.01$; **$P < 0.0001$ compared to *Cam*^{7}.

duced the same shortened, highly indented pupal cases seen with the *Cam*^{7} mutation. Ryanodine interacts very specifically with the ryanodine receptor, the major calcium-release channel of muscles. The action of ryanodine on the channel is complex, but at intermediate doses, the channel is locked into a subconductance state characterized by very long-lived openings (Meissner 1986; Lai *et al.* 1989).

Calcium release into the sarcoplasm involves a physical interaction between the L-type voltage-gated Ca^{2+} channel, the DHPR (Catterall 2000), of the plasma membrane and the RyR on the sarcoplasmic reticulum. The excitatory depolarization of the plasma membrane produces conformational changes in the DHPR, which in turn induce opening of the RyR channels. In skeletal-type muscles, which include the Drosophila larval body-wall muscles, calcium entry through the DHPR channels is not required to induce contraction. Thus, the RyR channels produce the major flux of calcium that triggers muscle contraction.

The fact that injection of ryanodine can phenocopy the *Cam*^{7} pupariation defect strongly suggests that abnormal calcium release in the muscles underlies this defect. Further, given that CaM is known to inhibit both RyR and DHPR channels at high calcium levels (Teng *et al.* 2002), this finding suggests that defective calcium release might result from defective regulation of one or both of these targets in the *Cam*^{7} mutant. A mutation (*Ryr*^{16}) in the single Drosophila RyR gene (Takeshima *et al.* 1994) is known to affect muscle function, producing lethality in the first instar (Sullivan *et al.* 2000). Mutations have also been identified in the gene encoding the pore-forming subunit of the DHPR channel, *Ca-α1D*, of the larval muscles (Eberl *et al.* 1998; Ren *et al.* 1998). Null *Ca-α1D* mutations die at hatching from failure of the muscle contractions needed to inflate the tracheae. Weaker mutations produce some adults, but the muscle contractions required for wing expansion always fail. We reasoned that if abnormally increased calcium levels underlie the *Cam*^{7} pupariation defects, reducing the number of functional RyR or DHPR channels might ameliorate the situation. We therefore examined *Cam*^{7} mutant animals heterozygous for mutations in either *Ryr* or *Ca-α1D*.

The *Ryr*^{16} mutation is not a null (Sullivan *et al.* 2000), so we also used deletion *Df(2R)H3E1*, which completely removes *Ryr*. The presence of one copy of the *Ryr*^{16} mutation produced a striking rescue of the *Cam*^{7} pupal and lethal phenotypes (Figure 4 and Table 2). The pupae (termed here *Ryr*^{16} *Cam*^{7} pupae) were smooth and indentation free in the anterior with only mild ridges in the posterior (Figure 4A). Their length:width ratios were actually higher than those of wild type (Figure 4B). While none of the *Cam*^{7} pupae eclose, >40% of the *Ryr*^{16} *Cam*^{7} animals emerged as adults, and those failing to eclose showed no head defects (Table 2). Interestingly, some of the eclosed *Ryr*^{16} *Cam*^{7} adults showed failed wing expansion as seen for weak *Ca-α1D* mutations. All of the eclosed adults performed poorly in the climb test, like the *Cam*^{7} animals rescued by muscle expression of wild-type CaM (see above). In marked contrast to *Ryr*^{16}, the *H3E1* deletion produced much smaller alleviation of the *Cam*^{7} phenotype. *H3E1* heterozygous pupae (*H3E1 Cam*^{7} pupae) showed some increase in the pupal length:width ratio (Figure 4B), but very few pupal cases showed decreased indentations. Fewer head defects were seen among the *H3E1 Cam*^{7} pharate adults (Table 2), but none were able to eclose (Table 2).

Controls were performed to investigate the unexpected difference in behavior between *Ryr*^{16} and the *H3E1* deletion. Since *Ryr* is on the second chromosome as is *Cam*, the *Ryr*^{16} and *H3E1* mutations were recombined onto the *Cam*^{7} chromosome (see materials and methods). Thus, an alternative explanation for this difference could be that the *Cam*^{7} phenotype is partially due to a second mutation on the *Cam*^{7} chromosome that was recombined away in generating the *Ryr*^{16} *Cam*^{7} chromosome but not the *H3E1 Cam*^{7} chromosome. To address this possibility, we examined five different recombinant *Ryr*^{16} *Cam*^{7} chromosomes and four *H3E1 Cam*^{7} chromosomes and found that all the recombinant chromosomes of the same type behaved identically. Thus, random differences in the chromosome regions ex-

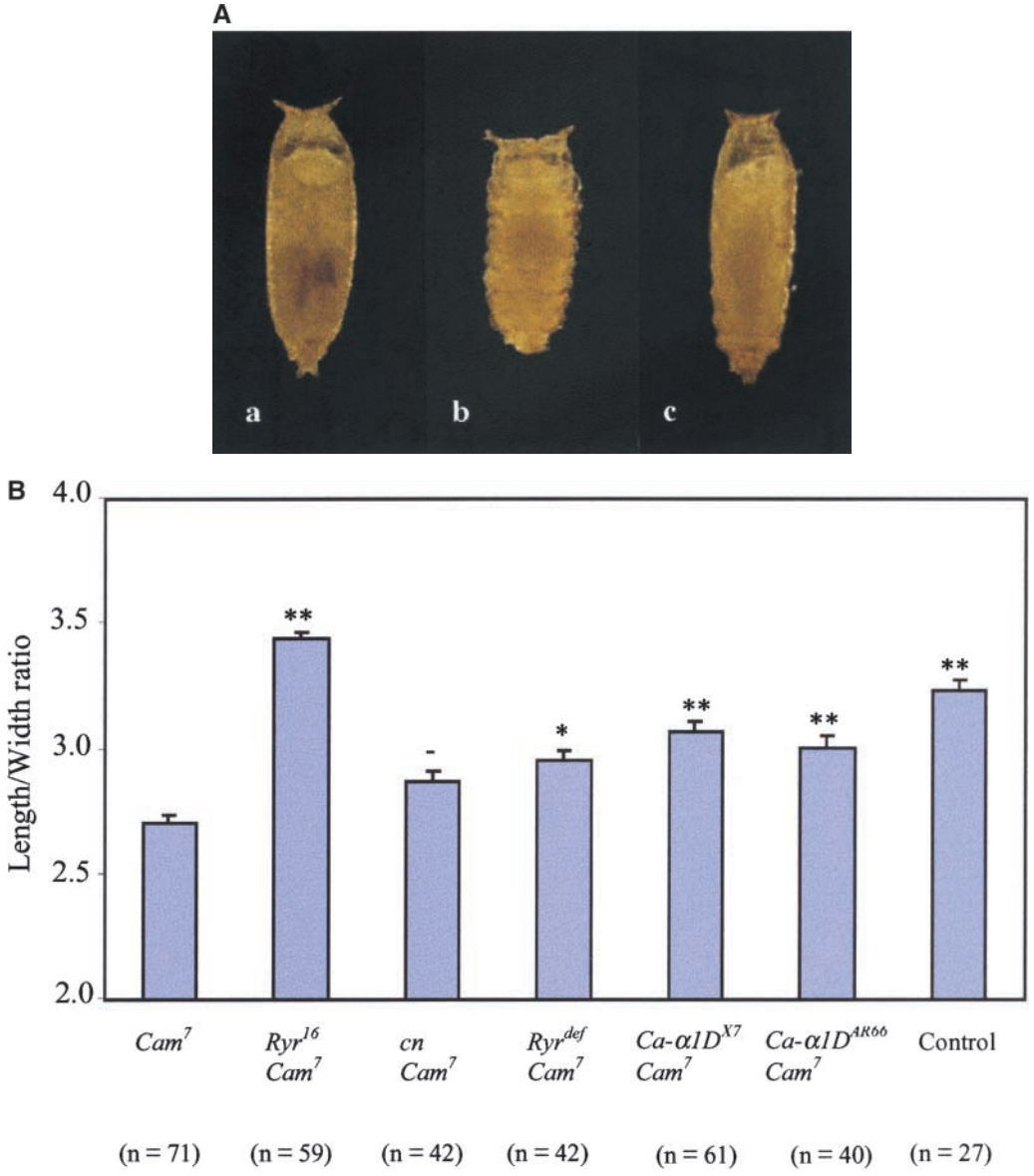

FIGURE 4.—Rescue of the *Cam*^{7} pupal case phenotype by introduction of one copy of an *Ryr* or *Ca-α1D* mutation. (A) Rescue of the *Cam*^{7} pupal case indentations by introduction of one copy of the *Ryr*^{16} mutation. (a) Control, *y w; + / Cam*^{n339}. (b) *Cam*^{7} pupal case, *y w; Cam*^{7}*/Cam*^{n339}. (c) *Ryr*^{16} *Cam*^{7} pupal case, *y w; Ryr*^{16} *Cam*^{7}*/Cam*^{n339}. Note that only mild indentations are present in the posterior half of *Ryr*^{16} *Cam*^{7} pupal cases. (B) Effects of mutations on pupal length:width ratios. Genotypes are as follows: *Cam*^{7}, *y w; Cam*^{n339}*/Cam*^{7}. *Ryr*^{16} *Cam*^{7}, *y w; Cam*^{n339}*/Ryr*^{16} *Cam*^{7}. *cn Cam*^{7}, *y w; Cam*^{n339}*/cn*^{1} *Cam*^{7}; *Ryr*^{def} *Cam*^{7}, *y w; Cam*^{n339}*/Df(2R)H3E1 Cam*^{7}. *Ca-α1D*^{X7} *Cam*^{7}, *y w; Cam*^{n339}*/Ca-α1D*^{X7} *Cam*^{7}. *Ca-α1D*^{AR66} *Cam*^{7}, *y w; Cam*^{n339}*/Ca-α1D*^{AR66} *Cam*^{7}. Control, *y w; Cam*^{n339}*/+*. $^{**}P < 0.0001$; $^{*}P < 0.01$; –, not significant; *n*, number of animals measured.

changed during recombination did not affect either phenotype. As a further test, an unrelated mutation, *cn*, which affects eye color, was recombined onto the *Cam*^{7} chromosome. *cn* is located close to *Ryr* on chromosome 2 and a similar region of the *Cam*^{7} chromosome must be exchanged to introduce *cn* onto the *Cam*^{7} chromosome. Four recombinant *cn Cam*^{7} chromosomes were examined and none showed any effects on the *Cam*^{7} mutation (Table 2). As a final control, we demonstrated that chromosomes carrying the *Cam*^{7} mutation alone and displaying the original *Cam*^{7} phenotype could be recovered from one of the *Ryr*^{16} *Cam*^{7} chromosomes. The difference in alleviation of the *Cam*^{7} phenotype shown by *Ryr*^{16} and *H3E1* thus seems to reflect a real difference in the effects of the two mutations.

To examine the effects of reduced DHPR channel function, we used two *Ca-α1D* mutations, the strong mutation *X7*, which behaves as a null in larvae, and the weaker allele, *AR66*, containing a point mutation (EBERL *et al.* 1998). The heterozygous *Ca-α1D*^{X7} mutation produced a small but significant increase in the length:width ratio of the pupal cases (Figure 4B) but had no obvious effect on the pupal case indentations. This mutation also enabled a very small fraction of the *Cam*^{7} pupae to eclose as weak, uncoordinated adults with failed wing expansion (Table 2). The weaker *Caα1D*^{AR66} mutation increased the length:width ratio of the *Cam*^{7} pupal cases (Figure 4B) but none of these pupae eclosed (Table 2).

Effects of the *Cam*^{7} mutation on larval body-wall calcium fluxes in response to K contracture: To determine whether calcium fluxes are altered in *Cam*^{7} muscles, we used aequorin to monitor calcium release upon muscle depolarization. Aequorin, when bound to its cofactor coelenterazine, luminesces in response to calcium binding. UAS-aequorin under Gal4 control has been used in

TABLE 2

Developmental abnormalities caused by the *Cam*^{7} mutation are partially rescued by the *Ryr*^{16} mutation

Genotype	No. of larvae collected	Animals that pupariate (%)	Well formed[a] (%)	Malformed[b] (%)	No head eversion[c] (%)	Non-eclosed[d] (%)	Eclosed[e] (%)
Cam^{7}	84	78.6	13.1	16.7	9.5	29.3	0
Ryr^{16} *Cam*^{7}	270	94.1	91.6	0	0	0	42.0
cn Cam^{7}	285	80.1	19.9	18.4	18.4	16.2	0
Ryr^{def} *Cam*^{7}	198	77.8	31.3	17.2	10.6	18.6	0
Ca-α1D^{X7} *Cam*^{7}	87	83.9	64.4	6.9	8.0	4.6	3.4
Ca-α1D^{AR66} *Cam*^{7}	43	89.1	67.4	7.0	2.3	14.0	0
Cam^{+}	85	92.9	90.6	0	0	2.3	88.2

First instar larvae of the appropriate genotype were collected and examined throughout development. Genotypes are as follows: *Cam*^{7}, *y w; Cam*^{n339}*/Cam*^{7}. *Ryr*^{16} *Cam*^{7}, *y w; Cam*^{n339}*/Ryr*^{16} *Cam*^{7}. *cn Cam*^{7}, *y w; Cam*^{n339}*/cn Cam*^{7}. *Ryr*^{def} *Cam*^{7}, *y w; Cam*^{n339}*/Df(2R)H3E1 Cam*^{7}. *Ca-α1D*^{X7} *Cam*^{7}, *y w; Cam*^{n339}*/Ca-α1D*^{X7}*Cam*^{7}. *Ca-α1D*^{AR66} *Cam*^{7}, *y w; Cam*^{n339}*/Ca-α1D*^{AR66} *Cam*^{7}. *Cam*$^{+}$, *y w; Cam*^{n339}*/+*. For *Ryr*^{16} *Cam*^{7} and *cn Cam*^{7}, five lines of each genotype were tested. For *Ryr*^{def} *Cam*^{7} , four lines were tested.

[a] Animals that have well-formed pupal head structures but are unable to eclose.

[b] Non-eclosed animals with malformed pupal heads.

[c] Non-eclosed animals with no head eversion.

[d] Non-eclosed animals that die before adult head development.

[e] Animals that eclose as adults.

Drosophila to examine calcium fluxes in the adult brain (Rosay *et al.* 2001) and Malpighian tubules (Rosay *et al.* 1997). We expressed aequorin in the muscles of *Cam*^{7} and control larvae and induced calcium release in preparations of body-wall muscles with high external [K^+] (K contracture; Hodgkin and Horowicz 1960).

Preliminary experiments were performed to identify a method of increasing [K^+] that produced synchronized depolarization of all muscle groups in the larval body wall. By rapidly introducing a large volume of high [K^+] solution, luminescence transients could be produced that had a single peak and a time frame comparable to those recorded in single fiber studies (Taylor *et al.* 1982). To allow for the variation in the expression of aequorin in individual animals, depolarization-induced luminescence was corrected for each animal to its individual baseline luminescence level. Thus these experiments did not address resting calcium levels in control or *Cam*^{7} animals. Figure 5A shows three superimposed luminescence transients for control larvae; these transients increased rapidly to a maximum and returned smoothly and sharply to baseline within 10 sec. Figure 5B shows transients for three *Cam*^{7} larvae; the rise in luminescence was not as rapid or as great and, most strikingly, the decline to baseline was slow and interrupted by secondary peaks. In these larvae, a complete return to baseline is not achieved even 50 sec after initial depolarization. These altered features of the *Cam*^{7} luminescence transients suggest three abnormalities in the *Cam*^{7} muscles: (i) loss of synchrony of calcium release in response to depolarization, (ii) lower overall calcium release, and (iii) failure of the mechanisms that inhibit calcium release quickly after depolarization.

Rescue of the backward movement phenotype in *Cam* null animals by neuronal expression of wild-type CaM: The phenotype of the *Cam* null mutation is very different from that of the *Cam*^{7} point mutation. As discussed above, *Cam* null animals die in the first instar showing behavioral abnormalities, the most pronounced of which is spontaneous backward locomotion. The one phenotypic characteristic shared with *Cam*^{7} animals is sluggishness. We investigated the tissue of origin of these two *Cam* null phenotypes with the same Gal4 drivers used for the *Cam*^{7} experiments.

Expression of wild-type CaM in the musculature did not rescue the backward movements or overall sluggishness of *Cam* nulls. In contrast, the backward movement was efficiently rescued by neural expression of CaM with a concomitant increase in forward movement (Figure 6). The larvae were still sluggish, however, with a BWC rate of ~40% that of controls. Significantly, the *sca*-Gal4 driver, which gives neural expression only between embryonic stages 6–14 (Mlodzik *et al.* 1990), produced no rescuing effect (Figure 6). As discussed earlier, all embryonic CaM is maternally derived, and zygotic protein appears not to be required until the perihatching period. The findings for the *sca*-Gal4 driver are consistent with this hypothesis and support the idea that the backward movement of *Cam* nulls is caused by neuronal defects after hatching and not by developmental problems.

Although the N- and C-terminal globular domains of CaM are similar, there is evidence that the two domains have discrete functions in target regulation (see Introduction). We recently discovered that muscle-specific expression of a mutant CaM with the two C-terminal Ca^{2+}-binding sites inactivated (termed B34Q) exacerbates the *Cam*^{7} phenotype, producing hypercontraction and larval death (Wang *et al.* 2002). In contrast, a mutant CaM with the two N-terminal Ca^{2+}-binding sites

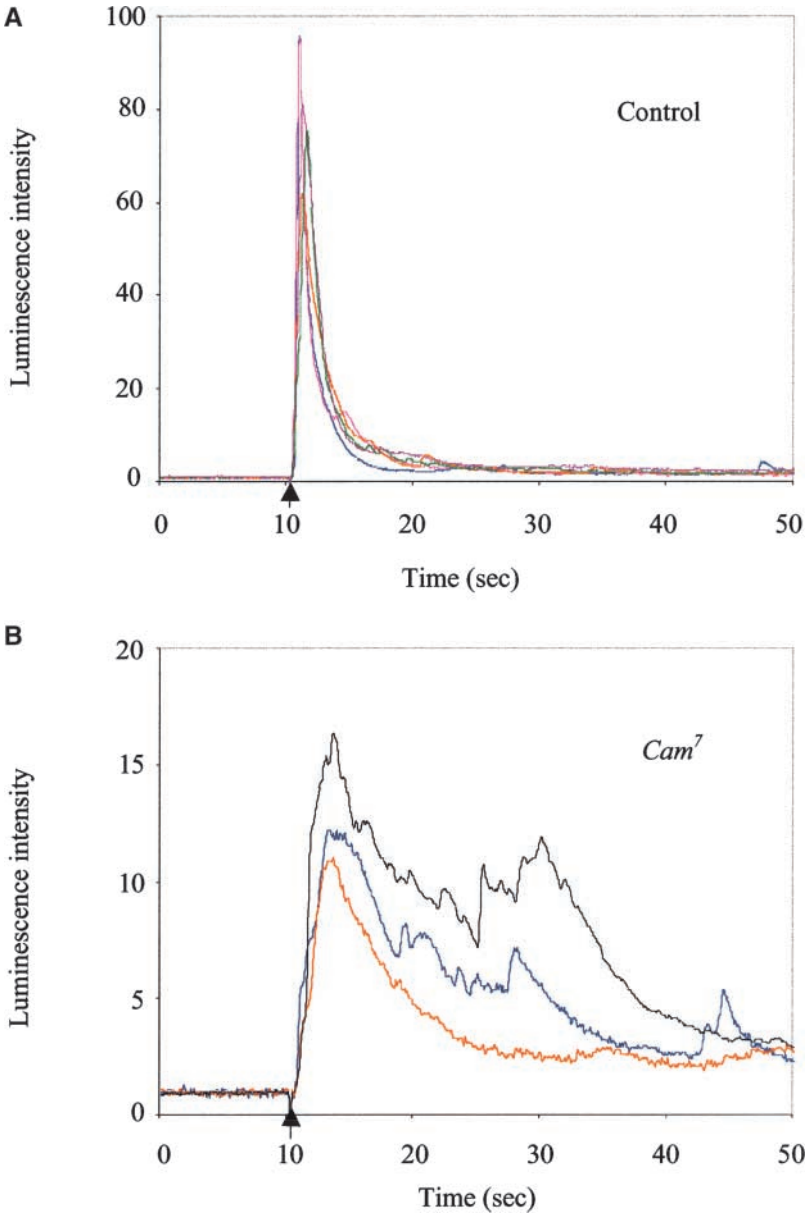

FIGURE 5.—Aequorin luminescence transients in control and *Cam*^{7} larval body-wall muscles. Aequorin transients produced by rapid high [K^+]-induced depolarization are shown. Transients for three control larvae (A) and three *Cam*^{7} larvae (B) are shown superimposed on one another. Arrow indicates the time of high [K^+] solution application.

inactivated (termed B12Q) produces an opposite effect; the *Cam*^{7} pupariation phenotype is "overrescued" and unusually long, smooth pupal cases are produced. A CaM with all four Ca^{2+}-binding sites inactivated (B1234Q) has little effect on the *Cam*^{7} phenotype. As a further approach to comparing the affected targets in *Cam*^{7} and *Cam* null animals, we examined the ability of these binding site mutants to rescue the backward movement of *Cam* null larvae when expressed in the nervous system. Interestingly, none of them could rescue the backward movement (Figure 7). This result indicates that different CaM target(s) are compromised in the *Cam* null mutant as compared to the *Cam*^{7} mutant and that the *Cam* null target(s) require fully calcium-saturated CaM for normal regulation. The *Cam*^{7}-encoded CaM (V91G CaM) rescues the *Cam* null defects as efficiently as wild-type CaM when expressed in the nervous system, providing further proof that different targets are affected by the *Cam* null and *Cam*^{7} mutations.

Light-induced spontaneous backward movements in hypomorphic *Cam* mutants: In addition to backward movements, *Cam* null larvae show increased head swinging (HEIMAN *et al.* 1996). Recently, the Campos laboratory (BUSTO *et al.* 1999) established that head swinging represents the first component of an aversion response to light. We therefore investigated the role of light in backward movement by *Cam* mutant larvae. As shown in Figure 8, backward movement in *Cam* null larvae is only slightly increased by high light levels. High light intensity could not induce backward movement in any of the single amino acid mutations of *Cam*, including *Cam*^{7} (Figure 8), or in wild-type larvae. However, for two hypomorphic mutants, *Cam*^{352} and *Cam*^{3909}, backward movements are significantly increased by high light in-

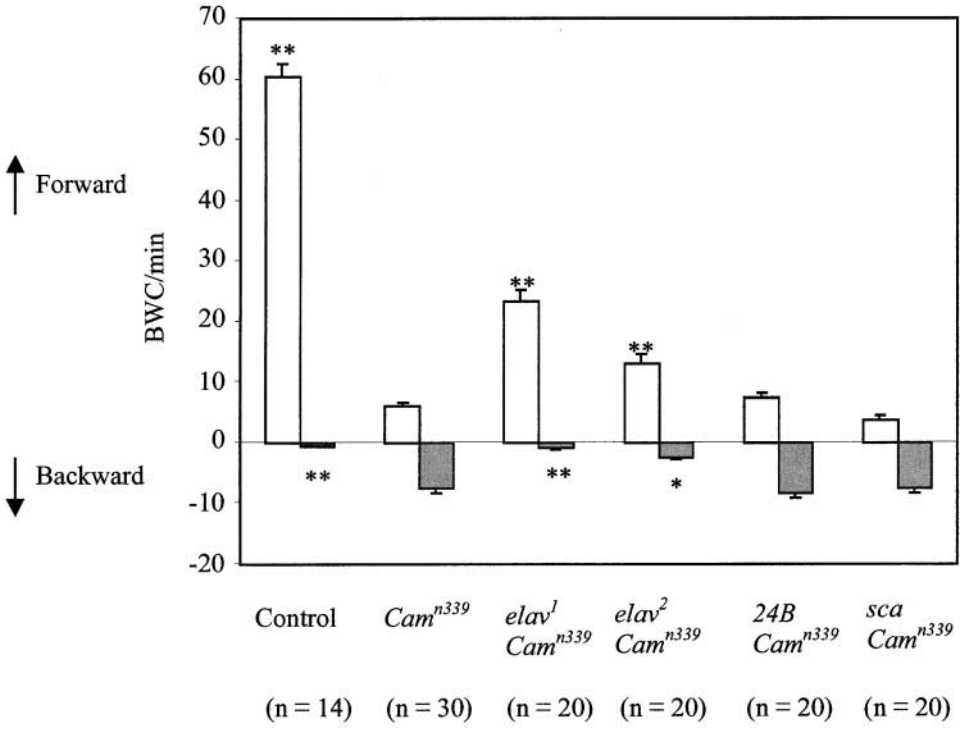

FIGURE 6.—Rescue of spontaneous backward movements in *Cam* null larvae by neuronal expression of wild-type CaM. Expression of wild-type CaM in the nervous system with the *elav*-Gal4 driver, but not the *sca*-Gal4 driver, reduces backward movement and increases forward movement in *Cam* nulls. Expression of wild-type CaM in the musculature under the 24B driver has no effect. Genotypes are as follows: Control, *y w; Cam^{n339}/+. Cam^{n339}, y w; Cam^{n339}. elav^{1} Cam^{n339}* (*elav* insertion on chromosome 2), *y w; Cam^{n339} elav-Gal4/Cam^{n339}; +/UAS-CaM. elav^{2} Cam^{n339}* (*elav* insertion chromosome 3), *y w; Cam^{n339}; elav-Gal4/UAS-CaM.* 24B *Cam^{n339}, y w; Cam^{n339}; 24B/UAS-CaM. sca Cam^{n339}, y w; Cam^{n339} sca-Gal4/Cam^{n339}; +/UAS-CaM. n*, number of larvae assayed. *$P < 0.001$; **$P < 0.0001$. Error bar, standard error.

tensity. Hemizygous *Cam^{352}* larvae contain less than one-tenth the amount of CaM found in wild-type larvae (SCOTT *et al.* 1997). The *Cam^{3909}* mutation results from a *P*-element insertion upstream of the *Cam* transcription start site (HARVIE *et al.* 1998). It has a similar, although milder, phenotype to *Cam^{352}* and presumably also produces decreased levels of wild-type CaM.

DISCUSSION

The *Cam^{7}* phenotype: The goal of these studies was to gain insight into the *in vivo* functions of CaM by examining the differing phenotypes of Drosophila *Cam* null and *Cam^{7}* (V91G) mutations. Our studies demonstrate that the *Cam^{7}* lethal phenotypes arise specifically from defects in the larval musculature, since muscle, but not neural, expression of wild-type CaM rescues *Cam^{7}* animals to adulthood. Larval sluggishness is not rescued by muscle-specific expression of CaM, however, indicating some mutant effects in other tissues. The poor coordination shown by *Cam^{7}* adults rescued with muscle-specific CaM expression may also reflect *Cam^{7}* defects in nonmuscle tissues. However, the failed mating behavior seen in rescued males correlates well with the poor expression achieved in the Muscles of Lawrence using the 24B driver.

Theoretically, the *Cam^{7}* mutation could disrupt muscle function by affecting (i) muscle development and structure, (ii) the contraction mechanism itself, or (iii) excitation-contraction coupling. Our previous findings on the role of maternal CaM in embryogenesis (see Introduction) eliminate developmental defects as the underlying cause. We found structural abnormalities in the body-wall muscles of wandering *Cam^{7}* larvae, but these probably reflect secondary muscle damage or degeneration. Some mutations to the human RyR that produce calcium leakage into the muscles lead to degenerative changes producing so-called central core disease (LYNCH *et al.* 1999).

Mutations that disrupt the contraction mechanism *per se* produce pupariation defects that are the exact opposite of those produced by *Cam^{7}*—that is, flaccid, elongated pupal cases (BUNCH *et al.* 1998). The hypercontraction in *Cam^{7}* thus suggests that the contraction apparatus is intact, functional, and overactivated. This recognition, and the phenocopy induced by ryanodine, indicate that excess contraction due to increased calcium levels is the primary defect in *Cam^{7}* muscles.

We demonstrated that calcium release in the body-wall muscles just prior to pupariation is severely disrupted in *Cam^{7}* animals. Upon membrane depolarization, low levels of asynchronous calcium release that did not return to base line were observed. These results seem paradoxical given the excessive contraction seen in *Cam^{7}* animals. However, an incomplete return to baseline calcium levels with each successive contraction could lead to progressive calcium accumulation in the sarcoplasm and thus to hypercontraction. Our calcium measurement technique could not address resting calcium levels in individual animals, but the progressive failure of relaxation in *Cam^{7}* animals as they age through third instar is consonant with this possibility. Further, over the lifetime of the animal this effect would slowly deplete the calcium stores so that by late third instar,

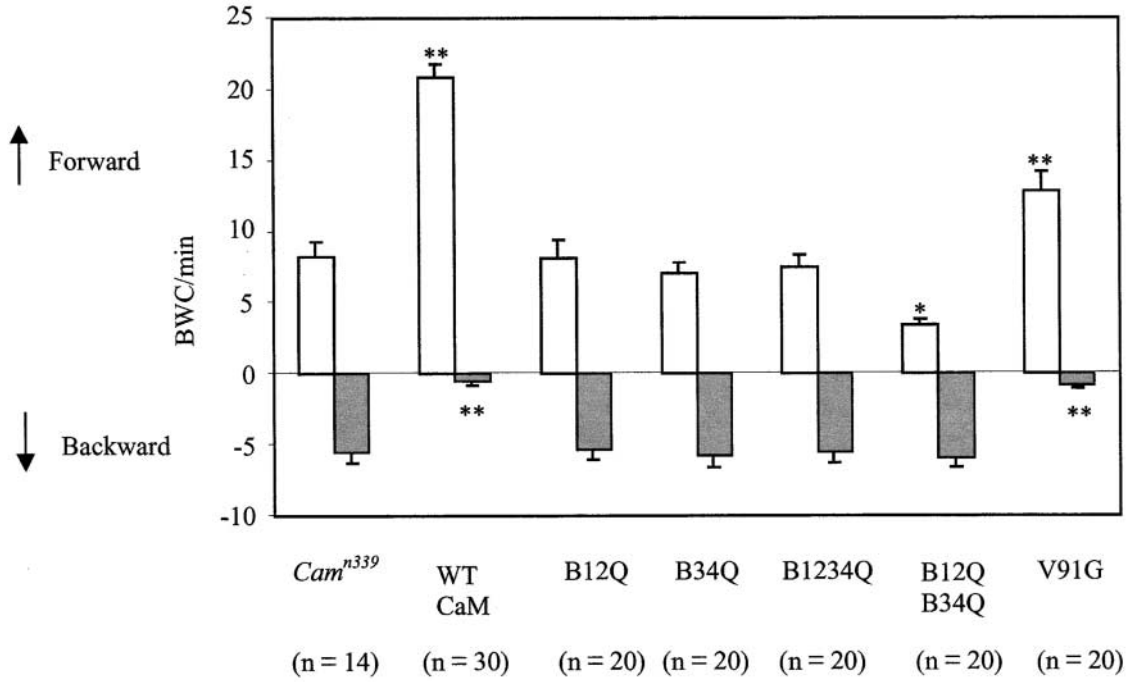

FIGURE 7.—Disruption of Ca^{2+}-binding by CaM abolishes its ability to rescue backward movement in *Cam* nulls. The rescue of backward movement seen when wild-type CaM (WT CaM) is expressed in the nervous system is lost when binding sites 1 and 2 (B12Q) or 3 and 4 (B34Q) or all four sites (B1234Q) are inactivated. Expression of two CaMs, one with sites 3 and 4 active (B12Q) and one with sites 1 and 2 active (B34Q), cannot compensate for wild-type CaM. In contrast, neural expression of V91G CaM does rescue the behavior. Genotypes are as follows: Cam^{n339}, as in Figure 6. WT CaM, as $elav^{1}$ Cam^{n339} in Figure 6. B12Q, B34Q, B1234Q, and V91G, as WT CaM except that UAS constructs expressing the appropriate mutant CaM were used. B12Q and B34Q, (*y w;* Cam^{n339} *elav-Gal4/*Cam^{n339} *UAS-B12Q; UAS-B34Q/+*). *, **, *n*, and error bars as in Figure 6.

when these assays were performed, calcium available for excitation-induced release would be significantly diminished.

In contrast to the hypercontraction at pupariation, the head eversion defects seen hours later are associated with failed muscle contractions. It is possible that by this stage permanent damage has occurred to the muscles. In adult insects, the calcium leakage caused by ryanodine produces muscle rigidity followed by progressive flaccid paralysis (JENDEN and FAIRHURST 1969). Alternatively, by this stage, the muscle calcium stores may be completely depleted and contraction may be impossible.

Both channel types responsible for calcium flux into the muscles (RyR and DHPR) are CaM-regulated proteins (reviewed in TENG *et al.* 2002) and thus are good candidates to be the target(s) affected by Cam^{7}. CaM regulation of RyR is relatively well-characterized. Each subunit of the tetrameric channel binds a single molecule of CaM, which regulates the channel in a biphasic manner. Ca^{2+}-free CaM (apoCaM) sensitizes the channel to opening at low calcium, whereas Ca^{2+}-bound CaM (holoCaM) inhibits channel opening, thus providing feedback regulation and channel closure after activity. CaM regulation of DHPR channels is less well investigated. In mammals, the α1 subunits of both skeletal- and cardiac-muscle DHPR channels bind CaM and, in the case of cardiac DHPRs, holoCaM mediates channel closure at high calcium. However, no equivalent studies have yet been reported for the skeletal α1 subunit.

The loss of prompt channel closure suggested by our aequorin experiments could thus reflect failed regulation of either RyR or DHPR channels. However, several factors suggest that the RyR is the target more affected by Cam^{7}. First, if CaM-induced closure of the RyR channels were still intact, then failed inactivation of the DHPR channels would have to override this functional, downstream regulation to keep the RyR channels open. In contrast, failed closure of the RyR channels would allow calcium to leak into the muscles independently of DHPR function.

Second, the tissue mRNA expression patterns for the two channels also point to a major role for the RyR. Embryonic expression of *Ryr* mRNA is primarily in the body wall and visceral musculature (SULLIVAN *et al.* 2000). Mosaic experiments with the Ryr^{16} mutation failed to reveal any roles for RyR in nonmuscle tissues during development (SULLIVAN *et al.* 2000). Thus, the rescue of the Cam^{7} phenotype by muscle expression of wild-type CaM is the expected result if RyR is the major target affected. In contrast, although *Dmα1D* encodes the α1 subunit of the L-type channel in larval muscles, the major site of mRNA expression in embryogenesis is the nervous system (ZHENG et al. 1995). Thus, if this

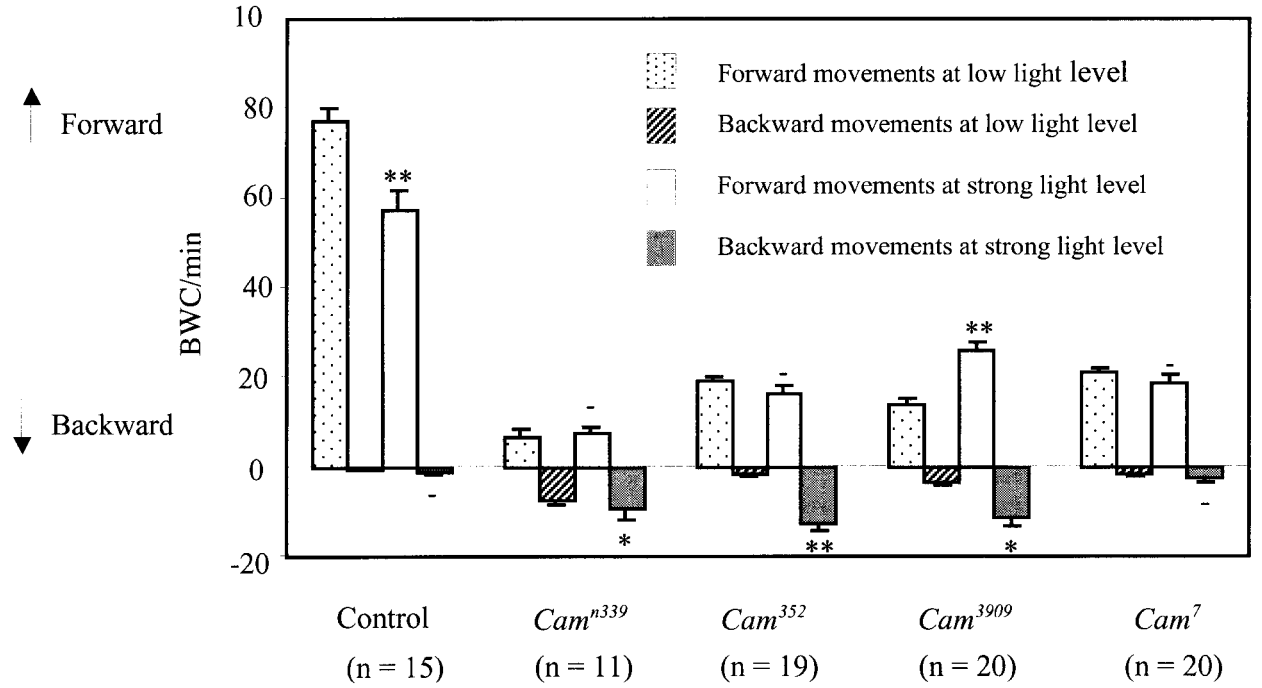

FIGURE 8.—Relationship between illumination and backward movement in *Cam* mutants. At low light intensity, the *Cam* hypomorphic mutants Cam^{352} and Cam^{3909} make almost no backward movements. At high illumination, both these mutants show robust backward movement. For control and Cam^{7} larvae, the presence or level of backward movement is unaffected by light. All mutations and the control chromosome were studied in the *y w* background, hemizygous to Cam^{n339}. *, **, *n*, and error bars as in Figure 6. –, not statistically significant.

DHPR channel were the major target affected by Cam^{7}, some component of the phenotype would be predicted to be neural in origin.

Our genetic interaction experiments also indicate that RyR is an important, if not the primary, muscle target affected by Cam^{7}. The Ryr^{16} mutation produces a remarkable suppression of the Cam^{7} phenotype. Almost half of the Cam^{7} animals are rescued to become morphologically normal adults. The ability of Ryr^{16} to rescue Cam^{7} more dramatically than an *Ryr* null mutation probably reflects the fact that each RyR channel is a tetramer. Whereas a heterozygous deletion will result in 50% fewer wild-type channels, a heterozygous mutant protein, assuming it can be incorporated into tetramers, will represent one or more subunits in 15 of 16 of all channel tetramers. Ryr^{16} is not dominant and thus its dramatic effect on the Cam^{7} phenotype suggests that (i) V91G CaM has an altered interaction with the wild-type RyR channels and (ii) when most of the channels contain at least one Ryr^{16} type subunit, the effects of that altered interaction are alleviated. It will be of interest to determine the extent to which calcium transients are restored in the Ryr^{16} Cam^{7} larvae. The protein encoded by the Ryr^{16} allele has not been characterized, although preliminary Western blot experiments indicate that it is similar in size to the wild-type protein (R. LIOU, K. M. C. SULLIVAN and K. BECKINGHAM, unpublished observations). The dynamics of CaM binding to the RyR are also not yet fully understood, although there is evidence that the conversion of CaM from an activator to an inhibitor upon calcium binding involves a shift in the position of CaM on RyR (RODNEY *et al.* 2001). Thus, more molecular work is required to explain the Ryr^{16}-Cam^{7} and Ryr^{+}-Cam^{7} interactions. We have evidence, however, that V91G CaM shows altered binding to one of the CaM-binding regions of RyR (B. WANG and K. BECKINGHAM, unpublished observations).

In addition to the two channels discussed above, misregulation of the calcium-ATPase (SERCA) pump that sequesters calcium into the sarcoplasmic reticulum could contribute to the Cam^{7} phenotype. In mammals, the cardiac muscle SERCA pump is activated by phosphorylation by CaM kinase II (TOYOFUKU *et al.* 1994). Failure of this activation would lead to accumulation of calcium in the muscles. However, in Drosophila, the CaM kinase II phosphorylation site is not conserved (SHI *et al.* 1998).

The *Cam* null phenotype: The spontaneous backward movement seen in *Cam* nulls clearly reflects target interaction defects that differ from those produced by Cam^{7}. The affected target(s) is neural, as opposed to muscular, and the requirements for rescue, in terms of functional calcium-binding sites on CaM, are different from those for rescue of Cam^{7}. As for the Cam^{7} mutation, however, the overall sluggishness of *Cam* nulls is not cleanly rescued by CaM expression in either neural or muscle tissue, reinforcing the idea that this defect reflects generalized loss of CaM.

The spontaneous backward movements of *Cam* null larvae seem compellingly similar to the enhanced backward swimming produced by C-terminal lobe CaM mutants in Paramecium (see Introduction). However, our experiments with versions of CaM defective in either N-terminal or C-terminal calcium binding indicate that the underlying target(s) in the two species show different regulation by CaM. Given that only C-terminal mutations produce exaggerated avoidance responses in Paramecium, a CaM with a functional C terminus might be expected to restore some functional interaction with a comparable target in Drosophila. But as shown in Figure 7, B12Q CaM is as ineffective as B34Q CaM in reducing backward movements.

Nevertheless, our findings on the influence of light on the *Cam* null phenotype suggest that, as in Paramecium, the defect results from hyperexcitability of the organism. Comparisons to the work of Busto *et al.* (1999) suggested that both the excessive head swinging and the backward movement seen in *Cam* nulls reflect components of a light-aversion response. Although head swinging in response to light is seen in control larvae, we could not induce backward movement in wild-type animals subjected to high light levels. In contrast, reduction of CaM protein levels in hypomorphic mutants produced light-induced backward movements, and in *Cam* null animals, this response seems to be constitutively activated. It is possible that the nervous system is extremely hypersensitive in *Cam* nulls and that even mild sensory input continuously triggers avoidance responses.

In Paramecium, *Cam* mutant-induced hyperexcitability results from failed regulation of a Ca^{2+}-activated repolarizing K^+ channel in the plasma membrane. Although differences in CaM target regulation are indicated by our experiments, defective control of key ion channels that regulate neuronal excitability seems likely to underlie the *Cam* null defect in Drosophila. Further experimentation will address this hypothesis.

We thank J. Douglas Armstrong for help with the luminometer experiments and Nam Ha, Isaac Sairs, Amanda Matthews, Lisa Whitmire, and Wiriya Chiranand for help with the behavioral studies and genetics. Sanford Bernstein generously provided the MHC-lacZ driver line. Susan Hamilton and George Rodney provided valuable discussion on the RyR and Ana Campos provided insightful advice on the role of light in larval behavior. This work was supported by the National Aeronautics and Space Administration Specialized Center of Research and Training in Gravitational Biology at Rice University and by a grant from the R. A. Welch Foundation of Texas (C-1119).

LITERATURE CITED

Arredondo, L., H. B. Nelson, K. Beckingham and M. Stern, 1998 Increased transmitter release and aberrant synapse morphology in a *Drosophila calmodulin* mutant. Genetics **150:** 265–274.

Brand, A., 1995 GFP in Drosophila. Trends Genet. **11:** 324–325.

Brand, A. H., and N. Perrimon, 1993 Targeted gene expression as a means of altering cell fates and generating dominant phenotypes. Development **118:** 401–415.

Bunch, T. A., M. W. Graner, L. I. Fessler, J. H. Fessler, K. D. Schneider *et al.*, 1998 The PS2 integrin ligand tiggrin is required for proper muscle function in Drosophila. Development **125:** 1679–1689.

Busto, M., B. Iyengar and A. R. Campos, 1999 Genetic dissection of behavior: modulation of locomotion by light in the *Drosophila melanogaster* larva requires genetically distinct visual system functions. J. Neurosci. **19:** 3337–3344.

Catterall, W. A., 2000 Structure and regulation of voltage-gated Ca^{2+} channels. Annu. Rev. Cell Dev. Biol. **16:** 521–555.

Chadfield, C. G., and J. C. Sparrow, 1985 Pupation in *Drosophila melanogaster* and the effect of the lethal cryptocephal mutation. Dev. Genet. **5:** 103–114.

Cyert, M. S., 2001 Genetic analysis of calmodulin and its targets in *Saccharomyces cerevisiae*. Annu. Rev. Genet. **35:** 647–672.

Doyle, K. E., G. E. Kovalick, E. Lee and K. Beckingham, 1990 *Drosophila melanogaster* contains a single calmodulin gene. Further structure and expression studies. J. Mol. Biol. **213:** 599–605.

Eberl, D. F., D. Ren, G. Feng, L. J. Lorenz, D. Van Vactor *et al.*, 1998 Genetic and developmental characterization of Dmcα1D, a calcium channel α1 subunit gene in *Drosophila melanogaster*. Genetics **148:** 1159–1169.

Fletcher, J. C., K. C. Burtis, D. S. Hogness and C. S. Thummel, 1995 The Drosophila E74 gene is required for metamorphosis and plays a role in the polytene chromosome puffing response to ecdysone. Development **121:** 1455–1465.

Geiser, J. R., D. van Tuinen, S. E. Brockerhoff, M. M. Neff and T. N. Davis, 1991 Can calmodulin function without binding calcium? Cell **65:** 949–959.

Hadorn, E., and H. Gloor, 1943 Cryptocephal ein spatt wirkender letalfaktor bei *Drosophila melanogaster*. Rev. Suisse Zool. **50:** 256–261.

Harvie, P. D., M. Filippova and P. J. Bryant, 1998 Genes expressed in the ring gland, the major endocrine organ of *Drosophila melanogaster*. Genetics **149:** 217–231.

Heiman, R. G., R. C. Atkinson, B. F. Andruss, C. Bolduc, G. E. Kovalick *et al.*, 1996 Spontaneous avoidance behavior in Drosophila null for calmodulin expression. Proc. Natl. Acad. Sci. USA **93:** 2420–2425.

Hess, N., W. A. Kronert and S. I. Bernstein, 1989 Transcriptional and post-transcriptional regulation of *Drosophila* myosin heavy chain gene expression, pp. 621–631 in *Cellular and Molecular Biology of Muscle Development*, edited by L. Kedes and F. Stockdale. A. R. Liss, New York.

Hewes, R. S., A. M. Schaefer and P. H. Taghert, 2000 The cryptocephal gene (ATF4) encodes multiple basic-leucine zipper proteins controlling molting and metamorphosis in Drosophila. Genetics **155:** 1711–1723.

Hodgkin, A. L., and P. Horowicz, 1960 Potassium contractures in single muscle fibres. J. Physiol. **153:** 386–403.

Jenden, D. J., and A. S. Fairhurst, 1969 The pharmacology of ryanodine. Pharmacol. Rev. **21:** 1–25.

Kink, J. A., M. E. Maley, R. R. Preston, K. Y. Ling, M. A. Wallen-Friedman *et al.*, 1990 Mutations in Paramecium calmodulin indicate functional differences between the C-terminal and N-terminal lobes in vivo. Cell **62:** 165–174.

Kovalick, G. E., and K. Beckingham, 1992 Calmodulin transcription is limited to the nervous system during Drosophila embryogenesis. Dev. Biol. **150:** 33–46.

Lai, F. A., M. Misra, L. Xu, H. A. Smith and G. Meissner, 1989 The ryanodine receptor-Ca^{2+} release channel complex of skeletal muscle sarcoplasmic reticulum. Evidence for a cooperatively coupled, negatively charged homotetramer. J. Biol. Chem. **264:** 16776–16785.

Ling, K. Y., M. E. Maley, R. R. Preston, Y. Saimi and C. Kung, 1994 New non-lethal calmodulin mutations in Paramecium. A structural and functional bipartition hypothesis. Eur. J. Biochem. **222:** 433–439.

Lynch, P. J., J. Tong, M. Lehane, A. Mallet, L. Giblin *et al.*, 1999 A mutation in the transmembrane/luminal domain of the ryanodine receptor is associated with abnormal calcium release channel function and severe central core disease. Proc. Natl. Acad. Sci. USA **96:** 4164–4169.

Meissner, G., 1986 Ryanodine activation and inhibition of the $Ca^{(2+)}$ release channel of sarcoplasmic reticulum. J. Biol. Chem. **261:** 6300–6306.

Mlodzik, M., N. E. Baker and G. M. Rubin, 1990 Isolation and

expression of *scabrous*, a gene regulating neurogenesis in Drosophila. Genes Dev. **4:** 1848–1861.

Nelson, H. B., R. G. Heiman, C. Bolduc, G. E. Kovalick, P. Whitley *et al.*, 1997 Calmodulin point mutations affect Drosophila development and behavior. Genetics **147:** 1783–1798.

Ohya, Y., and D. Botstein, 1994 Diverse essential functions revealed by complementing yeast calmodulin mutants. Science **263:** 963–966.

Ren, D., H. Xu, D. F. Eberl, M. Chopra and L. M. Hall, 1998 A mutation affecting dihydropyridine-sensitive current levels and activation kinetics in Drosophila muscle and mammalian heart calcium channels. J. Neurosci. **18:** 2335–2341.

Rodney, G. G., C. Porter Moore, B. Y. Williams, J.-Z. Zhang, J. Krol *et al.*, 2001 Calcium binding to calmodulin leads to an N-terminal shift in its binding site on the ryanodine receptor. J. Biol. Chem. **276:** 2069–2074.

Rosay, P., S. A. Davies, Y. Yu, A. Sozen, K. Kaiser *et al.*, 1997 Cell-type specific calcium signaling in a Drosophila epithelium. J. Cell Sci. **110:** 1683–1692.

Rosay, P., J. D. Armstrong, Z. Wang and K. Kaiser, 2001 Synchronized neural activity in the Drosophila memory centers and its modulation by *amnesiac*. Neuron **30:** 759–770.

Saimi, Y., and C. Kung, 1987 Behavioral genetics of *Paramecium*. Annu. Rev. Genet. **21:** 47–65.

Saimi, Y., and C. Kung, 2002 Calmodulin as an ion channel subunit. Annu. Rev. Physiol. **64:** 289–311.

Scott, K., Y. Sun, K. Beckingham and C. S. Zuker, 1997 Calmodulin regulation of Drosophila light-activated channels and receptor function mediates termination of the light response in vivo. Cell **91:** 375–383.

Shi, X., M. Chen, P. E. Huvos and P. M. D. Hardwicke, 1998 Amino acid sequence of a calcium transporting ATPase from the sarcoplasmic reticulum of the cross-striated part of the adductor muscle of the deep sea scallop: comparison to SERCA enzymes of other animals. Comp. Biochem. Physiol. **120:** 359–374.

Stewart, B. A., H. L. Atwood, J. J. Renger, J. Wang and C. F. Wu, 1994 Improved stability of Drosophila larval neuromuscular preparations in haemolymph-like physiological solutions. J. Comp. Physiol. [A] **175:** 179–191.

Sullivan, K. M., K. Scott, C. S. Zuker and G. M. Rubin, 2000 The ryanodine receptor is essential for larval development in *Drosophila melanogaster*. Proc. Natl. Acad. Sci. USA **97:** 5942–5947.

Takeshima, H., M. Nishi, N. Iwabe, T. Miyata, T. Hosoya *et al.*, 1994 Isolation and characterization of a gene for a ryanodine receptor/calcium release channel in *Drosophila melanogaster*. FEBS Lett. **337:** 81–87.

Taylor, S. R., J. R. Lopez, P. J. Griffiths, G. Trube and G. Cecchi, 1982 Calcium in excitation-contraction coupling of frog skeletal muscle. Can. J. Physiol. Pharmacol. **60:** 489–502.

Teng, W., S. Sencer and S. L. Hamilton, 2002 Calmodulin modulation of proteins involved in excitation-contraction coupling. Frontiers Biosci. **7:** 1583–1589.

Toyofuku, T., K. Kurzydlowski, N. Narayanan and D. H. MacLennan, 1994 Identification of Ser38 as the site in cardiac sarcoplasmic reticulum Ca^{2+}-ATPase that is phosphorylated by Ca^{2+}/calmodulin-dependent protein kinase. J. Biol. Chem. **269:** 26492–26496.

Van Eldik, L., and D. M. Watterson, 1998 *Calmodulin and Signal Transduction*. Academic Press, New York.

Van Houten, J., S. Y. Chang and C. Kung, 1977 Genetic analyses of "paranoiac" mutants of *Paramecium tetraurelia*. Genetics **86:** 113–120.

Wang, B., C. Bolduc and K. Beckingham, 2002 Calmodulin UAS constructs and the in vivo roles of calmodulin: analysis of a muscle-specific phenotype. Genesis **34:** 86–90.

Yao, K. M., and K. White, 1994 Neural specificity of elav expression: defining a Drosophila promoter for directing expression to the nervous system. J. Neurochem. **63:** 41–51.

Zdarek, J., and G. Fraenkel, 1972 The mechanism of puparium formation in flies. J. Exp. Zool. **179:** 315.

Zdarek, J., K. Slama and G. Fraenkel, 1979 Changes in internal pressure during puparium formation in flies. J. Exp. Zool. **207:** 187.

Zheng, W., G. Feng, D. Ren, D. F. Eberl, F. Hannan *et al.*, 1995 Cloning and characterization of a calcium channel alpha 1 subunit from *Drosophila melanogaster* with similarity to the rat brain type D isoform. J. Neurosci. **15:** 1132–1143.

Communicating editor: T. Kaufman